RESEARCH ARTICLE

Caspase-cleaved Amyloid Precursor Protein in Alzheimer's Disease

Carlos Ayala-Grosso[1]; Gordon Ng[2]; Sophie Roy[3]; George S Robertson[2]

[1] Department of Pharmacology, McGill University, Montreal, Canada.
[2] Department of Biochemistry and Molecular Biology and [3]Department of Pharmacology, Merck Frosst Centre for Therapeutic Research, Dorval, Quebec, Canada.

Caspase-3 mediated cleavage of the amyloid precursor protein (APP) has been proposed as a putative mechanism underlying amyloidosis and neuronal cell death in Alzheimer's disease (AD). We utilized an antibody that selectively recognizes the *neo* epitope generated by caspase-3 mediated cleavage of APP ($\alpha\Delta C^{csp}$-APP) to determine if this proteolytic event occurs in senile plaques in the inferior frontal gyrus and superior temporal gyrus of autopsied AD and age-matched control brains. Consistent with a role for caspase-3 activation in AD pathology, $\alpha\Delta C^{csp}$-APP immunoreactivity colocalized with a subset of TUNEL-positive pyramidal neurons in AD brains. $\alpha\Delta C^{csp}$-APP immunoreactivity was found in neurons and glial cells, as well as in small- and medium-size particulate elements, resembling dystrophic terminals and condensed nuclei, respectively, in AD and age-matched control brains. There were a larger number of $\alpha\Delta C^{csp}$-APP immunoreactive elements in the inferior frontal gyrus and superior temporal gyrus of subjects with AD pathology than age-matched controls. $\alpha\Delta C^{csp}$-APP immunoreactivity in small and medium size particulate elements were the main component colocalized with 30% of senile plaques in the inferior frontal gyrus and superior temporal gyrus of AD brains. In some control brains, $\alpha\Delta C^{csp}$-APP immunoreactivity appeared to be associated with a clinical history of metabolic encephalopathy. Our results suggest that apoptosis contributes to cell death resulting from amyloidosis and plaque deposition in AD.

Brain Pathol 2002;12:430-441.

Introduction

Amyloid plaques and neurofibrillary tangles that extend progressively to neocortical brain areas accompanied by an extensive synaptic and neuronal loss are prominent features of Alzheimer's disease (AD) (4, 5, 6). Programmed cell death or apoptosis has been proposed as a mechanism of neuronal cell death in acute and chronic neurological diseases including stroke, Parkinson's disease, amyotrophic lateral sclerosis, frontotemporal dementia (FTD), and AD (for review, see 21, 23, 27, 45).

In AD, a role for apoptosis is supported by studies linking AD-associated genes such as amyloid precursor protein (APP), presenilin 1, and presenilin 2 with neuronal cell death. (12, 13, 25, 42, 43; for review, see 22). Mutations in the secretase cleavage sequences of APP generate recognition sites prone to cleavage by caspases enzymes (8). Moreover, a caspase-cleaved APP proteolytic fragment called C31 that induces apoptosis in cell lines is elevated in AD brains (17).

Apoptosis effectors such as Bcl-2, Bcl-x, Bax, Bak, and Bad, as well as cysteine proteases such as caspase-2 (ICH-1) and caspase-3 (CPP-32) have been found to be up-regulated in AD (15, 20, 31). In addition, a variety of proteins responsible for structural and metabolic integrity have been shown to be substrates for caspase-3, suggesting a key role for this primary cell death effector protease in neuronal apoptosis in AD (19).

Senile plaques and neurofibrillary tangles as well as apoptotic-like mechanisms are present in AD, but the question of whether these features are causally related to cell death remains an unresolved issue. DNA fragmentation assessed by TUNEL labeling has been observed in AD brains (32, 35, 40). However, despite large numbers of cells with DNA fragmentation, only a few cells display the morphological characteristics of apoptosis such as membrane blebbing and chromatin condensation (16, 18, 40), or labeling for the c-jun/activating protein-1 (apoptosis-specific protein) (33). Furthermore, DNA fragmentation has also been observed in necrotic cells injured by oxidative damage (41) or by postmortem autolysis (33), indicating that this event is not a specific marker of apoptosis.

Increased expression of prostate apoptosis response-4 (Par-4) in a subset of neurons that show accumulations of abnormal tau protein is strong evidence that neuronal death in AD may be due to apoptosis (11). Besides, colocalization of neurofibrillary tangles and caspase-cleaved fodrin proteolytic fragments as well as active caspase-3 have been recently reported in AD brains (28, 37). In contrast, several studies have reported a lack of colo-

Corresponding author:
George S. Robertson, PhD, Director, Department of Pharmacology, Merck Frosst Centre for Therapeutic Research, C.P./P.O.Box 1005, Pointe Claire, Dorval, Quebec H9R 4P8, Canada (e-mail: George_Robertson@merck.com)

Patient	Age	Sex	PMI (h)	ApoE	Braak Index	Neuropathological Diagnosis
C1-9710	79	M	2.00	3/3	I	Control
C2-9714	76	M	2.50	3/3	I	Control
C3-9717	78	M	2.66	3/3	I	Control
C4-9639	73	F	2.50	3/3	I	Control
C5-9702	81	M	2.75	3/3	I	Control
C6-9833	82	F	2.00	3/3	I	Control
C7-9914	86	M	2.50	3/3	I	Control/small numbers of senile plaques and tangles
C8-9750	88	F	2.15	Nd	I	Control/Alzheimer type II glia, consistent with metabolic encephalopathy. Incidental Lewy bodies.
C9-9613	85	F	2.75	3/3	II	Control/spasmodic dysphonia
C10-9745	79	F	2.00	3/3	II	Control/
C11-9834	73	F	2.00	3/3	II	Control/ Alzheimer type II glia, consistent with metabolic encephalopathy
C12-9746	86	M	2.00	Nd	III	Control/mild amyloid angiopathy, focal concentration of diffuse plaques, Incidental Lewy bodies.
C13-9753	91	M	2.66	Nd	III	Control/sparse neocortical neuritic plaques and numerous neurofibrillary tangles.
C14-9819	87	F	2.00	3/3	III	Control
C15-9807	85	M	2.66	3/3	III	Control/sparse neocortical neuritic plaques and neurofibrillary tangles.
AD1-9751	84	M	3.00	3/3	III	Early Alzheimer's disease
AD2-9818	91	F	2.16	3/3	III	Early Alzheimer's disease
AD3-9822	90	M	2.50	3/3	III	Alzheimer's disease
AD4-9921	86	M	3.33	3/3	IV	Alzheimer's disease
AD5-9701	78	F	2.50	3/3	IV	Early Alzheimer's disease
AD6-9605	87	F	2.00	3/3	V	Alzheimer's disease
AD7-9609	75	M	2.50	3/3	V	Alzheimer's disease/Cerebral amyloid angiopathy
AD8-9626	85	M	3.25	3/3	V	Alzheimer's disease/seizure disorder
AD9-9642	85	M	14.66	3/3	V	Alzheimer's disease
AD10-9707	87	F	2.50	2/2	V	Alzheimer's disease
AD11-9725	88	M	1.75	3/3	V	Alzheimer's disease
AD12-9727	77	F	4.00	2/3	V	Alzheimer's disease
AD13-9733	85	M	2.33	3/3	V	Alzheimer's disease
AD14-9805	88	M	4.00	3/3	V	Alzheimer's disease
AD15-9828	84	F	2.00	3/3	VI	Alzheimer's disease
AD16-9812	84	M	4.33	Nd	VI	Alzheimer's disease

PMI: Postmortem interval in hours; ApoE: Apoliprotein genetic load; Nd: Not determined

Table 1. Age-matched control and AD case demographic information.

calization between neurofibrillary tangles and putative apoptotic markers such as DNA fragmentation (1, 16, 36). Furthermore, lack of active caspase-3 in AD (29) or exceptionally low numbers in Down syndrome (DS) autopsied brains (34) suggest that a specific role for caspase activation in neuronal death in AD is still unclear.

To further investigate whether caspase-cleaved APP is associated with the progression of amyloidogenesis in AD, we utilized immunohistochemical methodologies to determine the extent of colocalization of the caspase-3 cleaved APP fragment ($\alpha\Delta C^{csp}$-APP) and Aβ amyloid peptide in autopsied AD brains. Caspase-3 dependent processing of APP has been proposed as a putative mecha-

nism that may contribute to the amyloid burden and subsequent amplification of the apoptotic cascade in AD (8). If caspase activation contributes to AD pathology by generating a pro-amyloidogenic fragment such as $\alpha\Delta C^{csp}$-APP, we reasoned that there should be an increase in $\alpha\Delta C^{csp}$-APP immunoreactivity associated with senile plaques in AD brains.

We report here a significant association between $\alpha\Delta C^{csp}$-APP immunoreactive profiles and AD pathology. Consistent with this finding, $\alpha\Delta C^{csp}$-APP immunoreactivity was present in a subset of pyramidal neurons in early or advanced stage of DNA fragmentation and chromatin condensation in some cases of AD. In some age-matched control brains, elevated $\alpha\Delta C^{csp}$-APP immunoreactive elements were associated with a clinical history of metabolic encephalopathy rather than AD. These results suggest that apoptosis may contribute to the widespread cell death that occurs in AD.

Materials and Methods

Antibodies. The antibody directed against the caspase-cleaved APP neo-epitope, CHGV**VEVD**, $\alpha\Delta C^{csp}$-APP has been extensively characterized by Gervais et al (1999). This antibody was used at a dilution of 1:2000. A monoclonal antibody directed against amyloid $A\beta_{(1\text{-}12)}$ was used at a concentration of 1:2000 as previously described by Grant et al (2000). This antibody was kindly provided by A. C. Cuello (McGill University, Montreal, Canada). Glial fibrillary acidic protein (GFAP) was detected with a monoclonal antibody from Sigma Chemical Co. (St Louis, Mo) and used at a dilution of 1:2400. Active caspase–3 immunoreactivity was detected using a polyclonal purified rabbit antibody from Pharmingen (San Diego, Calif) at 1:2000. An enhanced Vectastain ABC Elite or ABC alkaline phosphatase kit was used from Vector Laboratories (Burlingame, Calif) to visualize $\alpha\Delta C^{csp}$-APP, $A\beta_{(1\text{-}12)}$ positive senile plaques and GFAP immunoreactivities. All other chemicals were of reagent grade and obtained commercially.

Human brain tissue. Brain tissues from the inferior frontal gyrus (IFG) and superior temporal gyrus (STG) were obtained at autopsy from 31 subjects, 16 clinically diagnosed and identified histopathologically as having AD (average age ± SEM = 84.6 ± 1.12 years, postmortem index mean 3.55 ± 0.76 hours) and 15 age-matched non-demented control subjects (81.9 ± 1.42 years; postmortem index = 2.34 ± 0.09 hours). Braak and Braak staging (2) was based on Gallyas (7), silver-pyridin Campbell-Switzer (3) and Thioflavine S staining methods. The human brain tissue used in this study was provided by the Sun Health Research Institute, (Sun City, Ariz). A demographic summary of these cases is presented in Table 1.

Immunoprecipitation of $\alpha\Delta C^{csp}$-APP from human brain. Tissue samples of the superior parietal cortex from at least 3 age-matched controls and 3 AD cases were homogenized in lysis buffer containing 50 mM Tris-HCl pH 7.4 (Gibco), 1% nonidet-40 (Sigma), 2 mM EDTA (Gibco), a minicomplete protease inhibitor cocktail (Roche) and 1 mM caspase-3 inhibitor. The homogenates were centrifuged at 16000 g (4°C) for 20 minutes. The supernatant was removed and precleared with protein A sepharose (Amersham) at 4°C for 1 hour. Precleared extracts were incubated at 4°C in a circular rotator with $\alpha\Delta C^{csp}$-APP antibody and protein A. Next, the samples washed at least 4 times with lysis buffer.

Samples were electrophoresed on a 6% Tris-glycine gel (Novex) for 120 minutes (110 V) and electrically transferred to a nitrocellulose membrane (0.45 μm pore size) overnight. Blots were then incubated for 2 hours with the anti-APP monoclonal antibody 22C11 (Chemicon) (diluted 1:2000 in 5% non-fat milk) and incubated with antirabbit horseradish peroxidase (Amersham), the immunoreactivity was detected with luminol (ECL, Amersham). Consistency of protein loading for each lane was verified by Ponceau red staining.

Immunohistochemistry. Autopsied brain tissues were snap frozen cryostat sectioned at 10 mm of thickness, mounted on superfrost slides and stored at -80°C until staining. Tissue sections were post fixed in 4% paraformaldehyde buffered with sodium phosphate (0.1 M, pH 7.4) at 4ºC for 5 minutes, then treated with 0.3% hydrogen peroxide in 100% methanol for 15 minutes at RT, and permeabilized with PBS (0.01 M) containing 0.1% Triton X-100 at RT for 30 minutes.

Nonspecific sites were blocked with 0.05% bovine serum albumin for 15 minutes and with 15% normal goat serum for 30 minutes. Slides were then incubated with the primary antibody at 4°C overnight. Biotinylated secondary antibodies (Vector Labs) at a dilution of 1:200 were applied for 1 hour at RT and immunoreactivity detected using diaminobenzidine (DAB) brown or alkaline phosphatase (AP) with DAB and AP substrate kits (Vector). No specific staining was detected on slides lacking the primary antibody. Slides from cases diagnosed with AD as well as age-matched controls were routine-

ly stained side by side in a single and double labeling paradigm using the same batch of antibodies.

We examined immunohistochemical labeling in cortical layers containing plaques and $\alpha\Delta C^{csp}$-APP immunoreactivity from 1 to 3 sections per brain sample. All histological and immunohistochemical images were acquired from a Zeiss Axioplan 2 microscope equipped with an Axiophoto 2 system adapted to a Sony 3 CCD DXC-950 color video camera. The video signal was routed via a Sony camera adaptor CMA-D2 into a microcomputer. Images were analyzed by a custom designed program implemented in Northern Eclipse, an image analysis system produced by Empix Imaging, Inc. (Mississauga, Ontario, Canada). Quantification of positive labeling was performed on longitudinal bands following a linear sampling pattern using a micrometer scale in the ocular as an external calibrator. Each determination represented the mean ± SEM of 20 measurements per brain section performed on different regions of the frontal and temporal cortices. The number of plaques and $\alpha\Delta C^{csp}$-APP profiles were counted over an area of 350 $\mu m \times 280$ μm.

Tunel labeling. A modified version of the TUNEL method originally described by Gavrieli et al (1992) was used in this study. In brief, free 3′OH DNA termini were labeled in situ with digoxigenin tagged nucleotides, which were then recognized by an anti-digoxigenin peroxidase antibody, that was visualized by bright field microscopy. TUNEL labeling was performed according to the Apoptag Plus Peroxidase In Situ Apoptosis Detection Kit (Intergen Company, Purchase, NY). Once the TUNEL procedure was performed, slides were then blocked with 15% normal goat serum (Vector) and incubated with $\alpha\Delta C^{csp}$-APP antibody at 4°C overnight. Biotinylated secondary antibodies (Vector Labs) at a dilution of 1:200 were applied for 1 hour at RT and immunoreactivity detected using diaminobenzidine (DAB) with a NovaRed kit (Vector). Slides from cases diagnosed with AD as well as age-matched controls were routinely stained side by side in a single and double labeling paradigm using the same batch of antibodies.

Data analysis. $\alpha\Delta C^{csp}$-APP immunoreactivity profiles appeared as multiple elements in AD and aged–matched control brains. These elements consisted of particulates that were small ($\alpha\Delta C^{csp}$-APPsp; 3 μm) or medium sized ($\alpha\Delta C^{csp}$-APPmp; 6 μm) or neuronal ($\alpha\Delta C^{csp}$-APPn) in nature. These elements were either

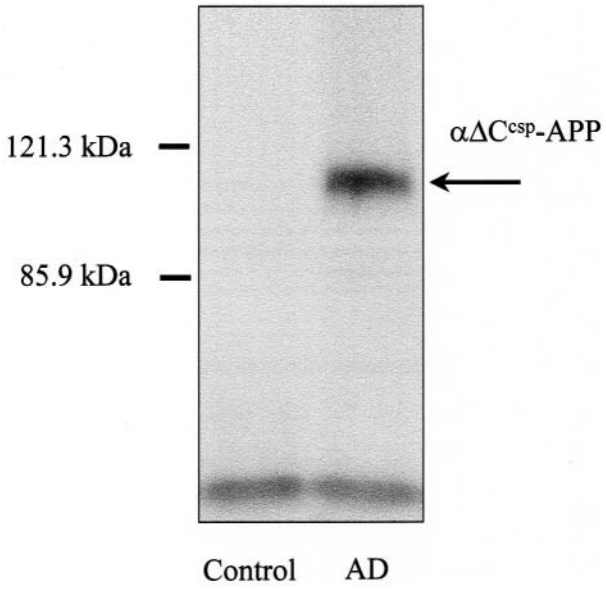

Figure 1. Immunoprecipitation of the caspase-cleaved amyloid precursor protein ($\alpha\Delta C^{csp}$-APP) proteolytic fragment from human brain. Tissue extracts of Parietal cortex from age-matched controls and AD patients were incubated 24 hours at 4°C with the $\alpha\Delta C^{csp}$-APP polyclonal antibody and protein A. Proteins immunoprecipitated were separated by sodium dodecyl-sulfate-polyacrylamide gel electrophoresis, transferred to nitrocellulose, and probed with the holo-amyloid precursor protein 22C11 monoclonal antibody. A prominent band at 116 kDa was detected in an AD brain extract.

associated ($\alpha\Delta C^{csp}$-APPpl$^+$) or unassociated with senile plaques ($\alpha\Delta C^{csp}$-APPpl$^-$).

Analysis of variance (ANOVA) mixed design (2 factor-within subjects, one factor-between subjects), was carried out to compare the mean density of $\alpha\Delta C^{csp}$-APPpl$^+$, $\alpha\Delta C^{csp}$-APPpl$^-$, $\alpha\Delta C^{csp}$-APPsp, $\alpha\Delta C^{csp}$-APPmp, and $\alpha\Delta C^{csp}$-APPn immunoreactive elements in the IFG and STG of AD and age-matched control brains. A statistical test was considered significant at $P<0.05$. Data analyses were performed using the SPSS statistical package (Version 10.0, 1998).

Results

The caspase-cleaved APP *neo*-epitope antibody ($\alpha\Delta C^{csp}$-APP) has been extensively characterized in vitro by Gervais et al (1999). In the present study, we detected caspase-cleaved APP proteolytic fragments in tissue extracts from parietal cortex of some cases of AD but not in age-matched controls (Figure 1). The $\alpha\Delta C^{csp}$-APP antibody recognized a protein approximately 110 kDa in size that corresponds to the molecular weight of APP processed by active caspase-3 as was reported by Gervais et al (1999). $\alpha\Delta C^{csp}$-APP (116 kDa) was pre-

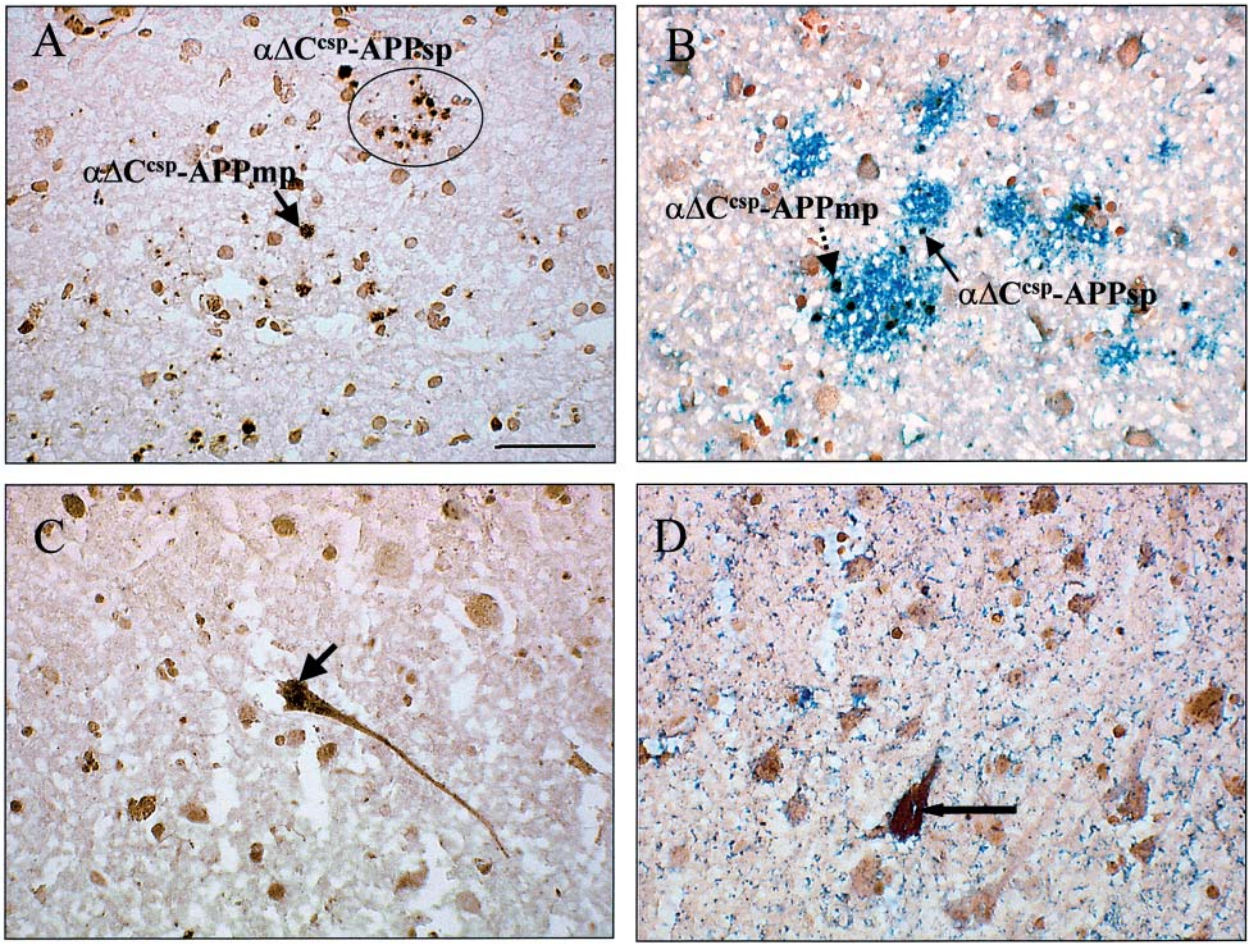

Figure 2. In age-matched control brains, small (αΔC^{csp}-APPsp, 3 μm, circle) and medium (αΔC^{csp}-APPmp, 6 μm, arrow) sized immunoreactive particulate elements were detected in a sparsely distributed fashion in the neuropile of all laminae of the frontal cortex (**A**), and in some diffuse amyloid plaques (**B**). In AD brains, pyramidal neurons were detected with the αΔC^{csp}-APP antibody (**C**, arrow), and in some cases αΔC^{csp}-APP immunopositives pyramidal neurons were found colocalized with intracellular Aβ (**D**, arrow). Scale bar = 50 μm.

dominant in 1 of 3 AD cases selected from our sample population.

Densities of αΔC^{csp}-APPmp and αΔC^{csp}-APPsp immunoreactive elements were consistently higher in AD that in age-matched control brains. αΔC^{csp}-APPmp and αΔC^{csp}-APPsp were round elements approximately 3 mm and 6 mm in diameter, respectively, with a size and morphologic appearance suggestive of dystrophic terminals and remnant nuclei (Figure 2A).

In a few control brains, αΔC^{csp}-APPmp and αΔC^{csp}-APPsp immunoreactive elements were colocalized with diffuse plaques (Figure 2B). Occasionally, αΔC^{csp}-APP immunoreactive pyramidal neurons were also found (results not shown). In AD brains, αΔC^{csp}-APPmp and αΔC^{csp}-APPsp immunoreactive elements were predominantly located in the middle and/or the periphery of diffuse and dense-core senile plaques (Figure 3B, C) and associated with dystrophic neurites (Figure 3B). In addition, αΔC^{csp}-APP immunoreactivity was found in neurons (Figure 2C; Figure 3A, B) and glial cells with astrocytic morphology (Figure 3A). In some AD cases, αΔC^{csp}-APP immunoreactivity was also colocalized with cell bodies containing intracellular Aβ (Figure 2D).

αΔC^{csp}-APP immunoreactivity was detected in pyramidal neurons associated with dense-core senile plaques (Figure 4A). However, αΔC^{csp}-APPmp and αΔC^{csp}-APPsp immunoreactive elements were the most common features detected in senile plaques (Figure 4B). In some cases, αΔC^{csp}-APP immunoreactivity was located in both neurons and GFAP positive cells in the absence of senile plaques (Figure 4C, D).

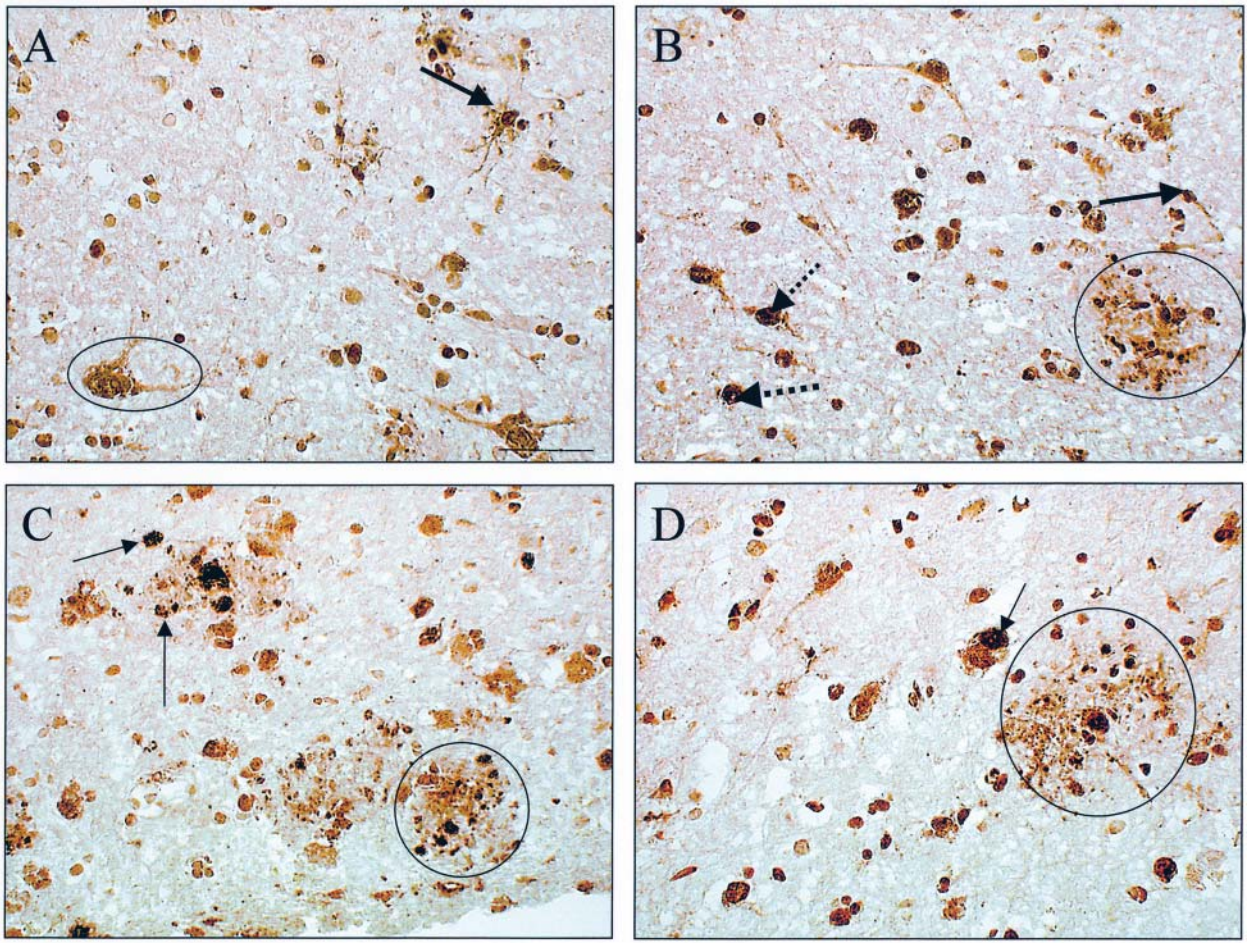

Figure 3. In AD brains, $\alpha\Delta C^{csp}$-APP immunoreactivity was found in the cytoplasm of multipolar neurons (circle) or astroglia (arrow) (**A**). $\alpha\Delta C^{csp}$-APP immunoreactive medium and small particulate elements were associated with remnant nuclei (**B**, broken arrows) and dystrophic neurites, respectively (**B**, arrow). $\alpha\Delta C^{csp}$-APP immunoreactive small particulates were also found in the middle and/or the periphery of diffuse plaques (**B, C, D**, circles) and in dense-core senile plaques (**C**, arrow). $\alpha\Delta C^{csp}$-APP immunoreactivity was also associated with and in the cytoplasm of neuronal cells as a component of granulovacuolar deposits (**D**, arrow). Scale bar = 50 μm.

Counts of neuritic plaques associated or unassociated with caspase-3 cleaved APP immunoreactive profiles, as well as counts of $\alpha\Delta C^{csp}$-APPn, $\alpha\Delta C^{csp}$-APPmp, and $\alpha\Delta C^{csp}$-APPsp immunoreactive components in the IFG and STG of AD and age-matched controls are shown in Figure 5. The density of senile plaques was considerably greater in AD brains than age-matched controls ($F = 71.97$, $df = 1$, $P < 0.0001$; Figure 5A). We found no difference in the number of neuritic plaques in the IFG and STG of AD brains. In the IFG and STG of AD patients, senile plaques that lacked $\alpha\Delta C^{csp}$-APP immunoreactive components ($\alpha\Delta C^{csp}$-APPpl-) were significantly more numerous than senile plaques containing $\alpha\Delta C^{csp}$-APP immunoreactive components ($\alpha\Delta C^{csp}$-$APPpl^{+}$) ($F = 13.41$, $df = 1$, $P = 0.001$).

Overall, densities of $\alpha\Delta C^{csp}$-APPn, $\alpha\Delta C^{csp}$-APPmp, and $\alpha\Delta C^{csp}$-APPsp immunoreactive elements were significantly higher in AD patients with respect to age-matched controls ($F = 40.50$, $df = 1$, $P < 0.0001$; Figure 5B). Similar numbers of $\alpha\Delta C^{csp}$-APP immunoreactive elements were found in the IFG and STG of AD brains. There was a positive association between $\alpha\Delta C^{csp}$-APP immunoreactive profiles and AD pathology ($F = 14.88$, $df = 2$, $P = 0.0001$).

We found elevated numbers of $\alpha\Delta C^{csp}$-APPn, $\alpha\Delta C^{csp}$-APPmp, and $\alpha\Delta C^{csp}$-APPsp in the IFG of some control cases with Alzheimer type II glia consistent with metabolic encephalopathy (C8-9750, C11-9834). This suggests that caspase-3 cleaved APP fragments can be generated

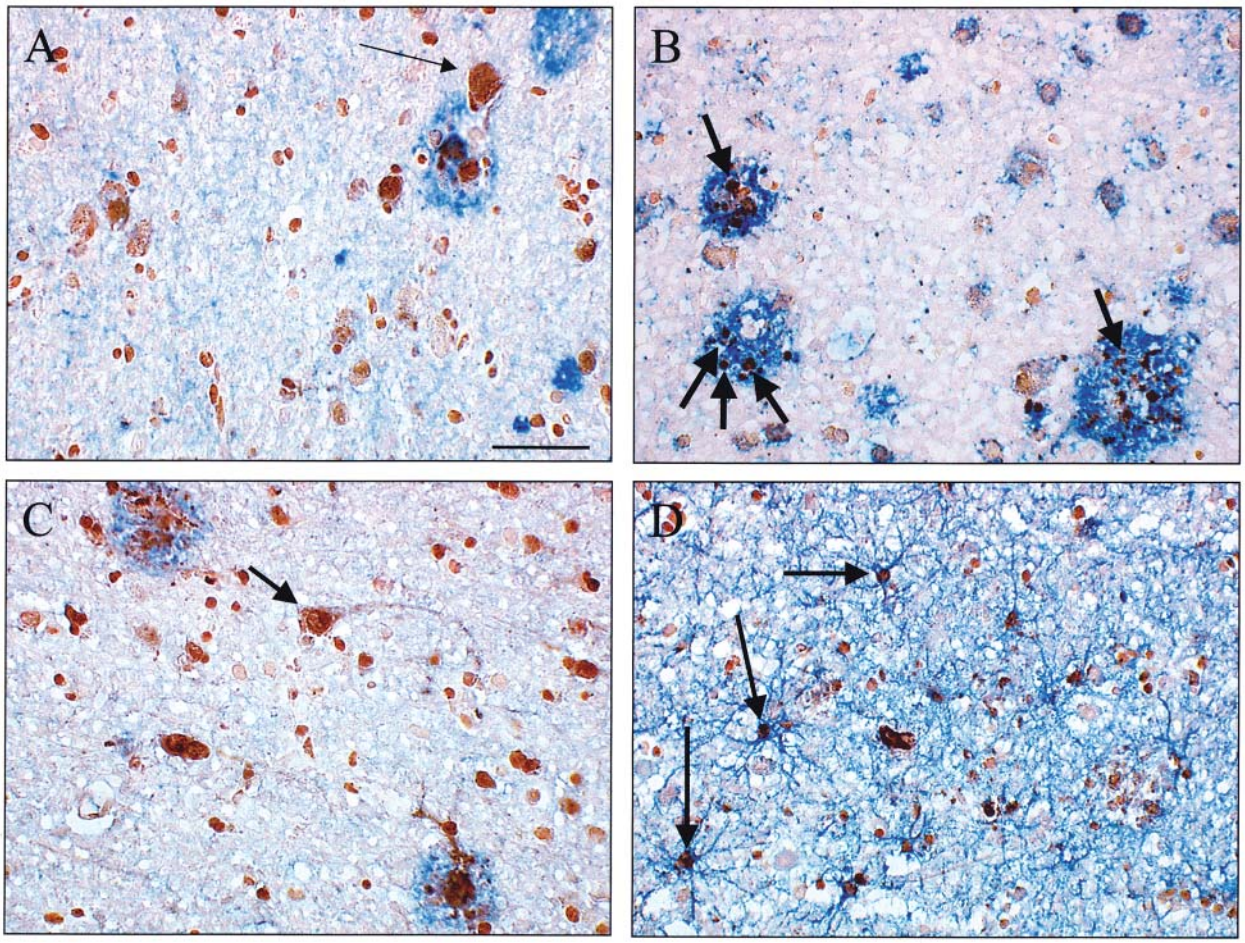

Figure 4. In AD brains, $\alpha\Delta C^{csp}$-APP immunoreactivity was detected in pyramidal neurons of the temporal cortex associated with some dense-core senile plaques (**A**, arrow), as well as in neurons (**C**, arrow) and GFAP positive cells (D, arrows) unassociated with senile plaques. $\alpha\Delta C^{csp}$-APPsp and $\alpha\Delta C^{csp}$-APPmp immunoreactivities were the main components found in mature non dense-core senile plaques (**B**, arrows). Scale bar = 50 μm.

in AD as a consequence of mechanisms that are independent of amyloidosis and plaque deposition.

By examining individual cases, we detected a remarkable elevation in the number of $\alpha\Delta C^{csp}$-APPn in some preclinical cases of AD diagnosed with mild amyloid angiopathy and an assigned Braak and Braak index of III (C12-9746, C13-9753). In contrast, the number of $\alpha\Delta C^{csp}$-APPn in AD brains was highly variable, and in some cases a few or no $\alpha\Delta C^{csp}$-APPn counts were observed, although these patients had been classified with a Braak and Braak index of V. These results suggest that $\alpha\Delta C^{csp}$-APP immunoreactivity is not correlated with the severity of pathology defined according to the Braak and Braak index. Furthermore, we found in sections from AD cases with elevated counts of $\alpha\Delta C^{csp}$-APPn, a lack of colocalization of $\alpha\Delta C^{csp}$-APPn with thioflavine S positive cells (results not shown), suggesting that neurofibrillary tangles and caspase-cleaved APP proteolysis may be independent events in AD.

TUNEL positive cells were rarely observed in age-matched controls (Figure 6A). In contrast, we found a relatively high number of cells undergoing DNA fragmentation and chromatin condensation in AD brains (Figure 6B, C arrows). Furthermore, we found that $\alpha\Delta C^{csp}$-APPn immunoreactivity colocalized with a subset of TUNEL-positive pyramidal cells (Figure 6B, D circles).

Counts of $\alpha\Delta C^{csp}$-APPpl^{-} were significantly more numerous than $\alpha\Delta C^{csp}$-APPpl^{+} in the frontal and temporal cortices of AD brains. This result is consistent with the fact that approximately 70% of senile plaques in the IFG and STG of AD brains did not contain $\alpha\Delta C^{csp}$-APP immunoreactivity.

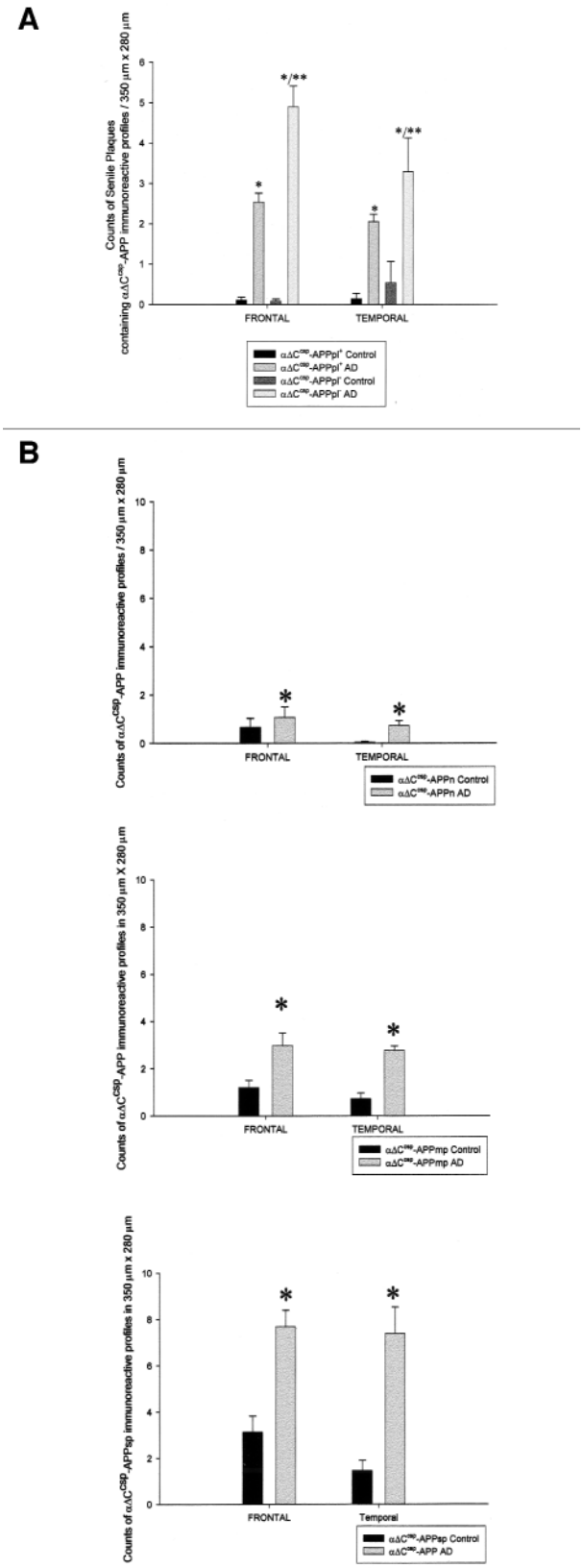

Figure 5. Counts (mean ± SEM) of senile plaques and αΔC^{csp}-APP immunoreactive elements in the inferior frontal gyrus and superior temporal gyrus of age-matched control (n = 12) and AD (n = 14) brains. Densities of senile plaques associated (αΔC^{csp}-APPpl^{+}) or unassociated (αΔC^{csp}-APPpl^{-}) with αΔC^{csp}-APP immunoreactive profiles are shown in **A**. Seniles plaques were significantly elevated in AD with respect to age-matched control brains (F = 71.97, df = 1, **P*<0.0001). In AD brains, senile plaques unassociated with αΔC^{csp}-APP were significantly higher with respect to senile plaques associated with αΔC^{csp}-APP in AD brains (F = 13.41, df = 1, ***P* = 0.001). Counts of αΔC^{csp}-APPn, αΔC^{csp}-APPmp, and αΔC^{csp}-APPsp immunoreactive profiles are shown in **B**. Overall, there was an elevated number of αΔC^{csp}-APP immunoreactive profiles in AD with respect to age-matched control brains (F = 40.57, df = 1, **P*<0.0001). A significant association between αΔC^{csp}-APP immunoreactive profiles with AD was determined (F = 14.89, df = 2, P = 0.0001).

In aged-matched control and AD brains (C1-9710, AD6-9605, AD13-9733, AD14-9805) we observed intraneuronal αΔC^{csp}-APP immunoreactivity. However, we found evidence for only weak active caspase-3 immunoreactivity in just a very few neuronal cell bodies in each of these cases (results not shown).

Discussion

In the present study, we examined the colocalization of caspase-cleaved amyloid precursor protein (αΔC^{csp}-APP) in neuritic plaques in the IFG and STG of AD and age-matched control brains.

Our antibody specifically recognizes a 116 kDa proteolytic fragment extracted from human parietal cortex of AD cases that corresponds with the predicted molecular weight of the caspase-cleaved amyloid precursor protein proteolytic fragment (αΔC^{csp}-APP). This result is consistent with previous in vitro findings where activation of caspase-3, as a consequence of apoptotic stimuli, may generate a similar fragment from APP during execution of the cell death program. Furthermore, accumulation αΔC^{csp}-APP is consistent with studies that have reported a significant increase of caspase-cleaved fodrin (28) and actin in AD brains (44).

In several control cases that demonstrated elevated numbers of αΔC^{csp}-APPmp immunoreactivity, there was an association with a clinical history of metabolic encephalopathy and stroke rather than AD. Elevated αΔC^{csp}-APP immunoreactivity in sections of age-matched controls may be the result of Alzheimer type II glia consistent with metabolic encephalopathy (C8-9750, C11-9834). In addition to the progression of AD pathology, a clinical history of ischemia (AD14-9805) may also contribute to elevated counts of αΔC^{csp}-APP immunoreactive components. Consistent with these findings, several reports have described elevated apop-

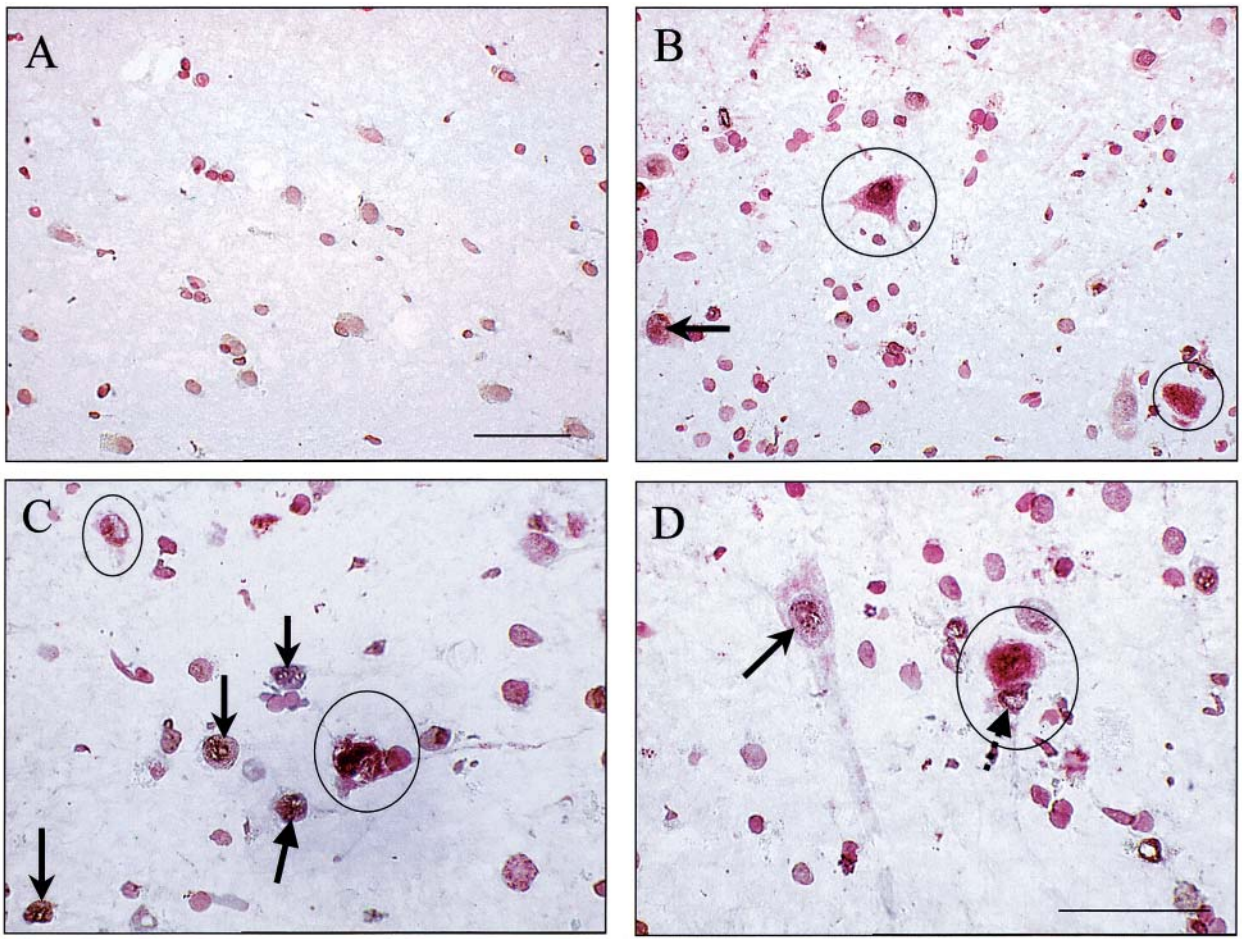

Figure 6. In age-matched control brains, we rarely found TUNEL-positive cells (**A**) Scale bar = 50 μm. In contrast, in AD brains we found a significant higher number of TUNEL-positive cells (**B, C, D**, arrows). We found αΔC^{csp}-APP immunoreactivity in a subset of pyramidal neurons of the temporal cortex colocalized with TUNEL-positive labeling (**B, C, D**, circles). Chromatin condensation can be seen in a neuron (**D**, circle, broken arrow). Scale bar in **D** = 50 μm.

tosis in aged-conditions or in pathologies not related to AD (20, 29, 37).

In this study, αΔC^{csp}-APP immunoreactivity colocalized with 30% of senile plaques in the IFG and STG of AD brains. αΔC^{csp}-APP immunoreactive small and medium size particulate elements were colocalized to a greater extent with early and mature plaques than in older dense-core plaques. These findings suggest that during the progression of AD pathology, amyloidosis and plaque deposition may promote caspase activation that triggers neuronal cell death, resulting in the accumulation of αΔC^{csp}-APP immunoreactive particulate elements in injured cells and dystrophic neurites. The clearance of αΔC^{csp}-APP immunoreactive profiles from older plaques may be responsible for the low incidence of αΔC^{csp}-APP labeling in dense-core plaques. An alternative explanation is that in late stages of AD, multiple neuromodulatory mechanisms may be disturbed as a consequence of amyloid burden and neurofibrillary tangles that may potentially lead to cell death by both apoptotic and non-apoptotic mechanisms.

The mean counts of αΔC^{csp}-APPn were highly variable in AD but they were more frequent in AD than age-matched control brains. In addition, we found a lack of colocalization between αΔC^{csp}-APPn and thioflavine S positive cells (results not shown). This finding is in agreement with reports indicating a mismatch between the distribution of TUNEL positive nuclei and senile plaques (40). Furthermore, it has been shown that amyloid burden is not correlated with either cell loss or neurofibrillary tangles (9). Therefore, the accumulation and subsequent deposition of amyloid Aβ peptide may be a risk factor rather than a primary mechanism of neurodegeneration in AD.

We found a higher numbers of TUNEL-positive cells in AD brains than age-matched controls. In addition, a subset of TUNEL-positive pyramidal cells colocalized with $\alpha\Delta C^{csp}$-APP immunoreactivity. Mismatches between the estimates of TUNEL-positive cells and $\alpha\Delta C^{csp}$-APPn immunoreactive profiles suggests that DNA fragmentation and chromatin condensation assessed by TUNEL seem to follow a temporal course different from that for activation of caspase-3, one of the key steps in apoptotic cell death.

$\alpha\Delta C^{csp}$-APPmp and $\alpha\Delta C^{csp}$-APPsp were the most frequent components in a subset of senile plaques containing $\alpha\Delta C^{csp}$-APP profiles. In these plaques, there may be at least 3 potential independent sources of $\alpha\Delta C^{csp}$-APP immunoreactivity: *i)* as a consequence of amyloidosis and plaque deposition as occurs in AD; *ii)* as a result of intracellular accumulation of Ab; or *iii)* subsequent to multiple local events occurring during senescence.

Our data support the hypothesis recently proposed by Terry (2000) in which a differential incidence in the cognitive impairment in AD may occur as a consequence of distinct pathological processes leading to the loss of synaptic and somatic neuronal components. Caspase-3 activation may produce localized synaptic loss and terminal dystrophy. For instance, $\alpha\Delta C^{csp}$-APPn, $\alpha\Delta C^{csp}$-APPmp and $\alpha\Delta C^{csp}$-APPsp immunoreactive elements may represent different stages of these events. This suggestion is supported by the detection of $\alpha\Delta C^{csp}$-APP immunoreactivity in neurons, and dystrophic neurites as well as in GFAP positive cells not associated with senile plaques. In the current study, an extensive accumulation of $\alpha\Delta C^{csp}$-APP immunoreactivity in neurons and glia in some cases of AD was not associated with senile plaques. This suggests that caspase activation occurs in multiple cellular components as discrete elements recruited by the amyloid burden in AD or in association with local pathologic events.

A role for glial cells in AD pathology is supported by studies that describe increased Fas antigen (CD95) expression in astrocytes and in a subpopulation of GFAP positive cells of AD brains (24). Kitamura et al (1997) have also shown an up-regulation of the tumor-suppressor protein p53 protein in glial cells of AD subjects.

The major argument for apoptotic cell death in AD is based primarily on an elevation of the number of cells with DNA fragmentation in AD brains relative to age-matched controls (16, 18, 32, 33, 35, 40). There are, however, reservations about the notion that cells with DNA fragmentation are actually apoptotic. Neurons with DNA fragmentation in AD do not show the classical morphological features of apoptosis, namely, chromatin condensation and nuclear fragmentation (26, 33). In our study, consistent with a role for caspase-3 activation in AD pathology, $\alpha\Delta C^{csp}$-APP immunoreactivity colocalized with a subset of TUNEL positive pyramidal neurons in IFG and STG of AD brains.

In the present study, we did not detect active caspase-3 in AD brains, although we found weak active caspase-3 like-immunoreactivity around plaques and some neuronal cell bodies in both AD and age-matched control as described by Su et al (2001). This may be due to the fact that active caspase-3 has a shorter half-life than caspase-cleaved proteolytic fragments such as $\alpha\Delta C^{csp}$-APP (8).

In 2 studies, active caspase-3 immunoreactivity has been recently reported in AD brains (34, 37). However, the number of active caspase-3 positive cells was not consistent in these 2 studies. Stadelmann et al (1999) reported an exceptionally low number of active caspase-3 positive cells in sections from AD and DS brains. Furthermore, a lack of colocalization of active caspase-3 with hyperphosphorylated tau was also found. In contrast, Su et al (2001), using the same antibody (CM1) that recognizes the p18 kDa component of active caspase-3 enzyme, have reported a significantly elevated number of active caspase-3 positive cells in AD brains colocalized with hyperphosphorylated tau. The explanation for these discrepancies is beyond the scope of the present study. However, differences in tissue processing (paraffin embedding versus post-fixed free-floating fresh frozen tissue) and counting methods may have contributed to these discrepant findings. Furthermore, Zheng et al (2000) have recently reported a lack of specificity of the CM1 antibody for active caspase-3 enzyme as a result of cross-reactivity with active caspase-6. These findings suggest that the presence of active caspase-3 in neurodegenerative pathologies such as AD remain to be convincingly shown.

Our study provides evidence of caspase-dependent proteolytic events during aging and AD pathology. We concluded that an accumulation of caspase-3 cleaved APP proteolytic fragments occurs in multiple cellular components in AD. This suggests that caspase activation may contribute to cell death in AD. However, whether activation of caspases initiates cell death in AD remains to be determined.

Acknowledgements

We wish to thank Francois Gervais (Merck-Frosst Centre for Therapeutic Research) for kindly providing the $\alpha\Delta C^{csp}$-APP antibody and Kevin Clark (Merck-Frosst

Centre for Therapeutic Research) for assistance with the figures. We are also grateful to A. C. Cuello (McGill University) for providing the $A\beta_{(1-12)}$ antibody. We are particularly indebted to the Sun Health Research Institute for providing us with Alzheimer's and aged-matched control brain sections for immunohistochemical analysis. C. Ayala-Grosso is a fellow of Consejo de Desarrollo Científico y Humanístico de la Universidad Central de Venezuela.

References

1. Bancher C, Lassmann H, Breitschopf H, Jellinger KA (1997) Mechanisms of cell death in Alzheimer's disease. *J Neural Transm Suppl* 50:141-152.
2. Braak H, Braak E (1991) Neuropathological stagging of Alzheimer-related changes. *Acta Neuropathol (Berl)* 82 :239-259.
3. Campbell SK, Switzer RC, Martin TL (1987) Alzheimer's plaques and tangles: A controlled and enhanced silver-staining method. *Soc Neurosci Abs* 13:678.
4. Cummings JL, Vinters HV, Cole GM, Khachaturian ZS (1998) Alzheimer's disease. Etiologies, pathophysiology, cognitive reserve and treatment opportunities. *Neurology* 51 (Suppl 1):S2-S17.
5. DeKosky ST, Scheff SW (1990) Synapse loss in frontal cortex biopsies in Alzheimer's disease: Correlation with cognitive severity. *Ann Neurology* 27:457-464.
6. Delacourte A, Sergeant N, Buee L, Wattez A, Vermersch P, Ghozali F, Fallet-Bianco C, Pasquier F, Lebert F, Petit H, Di Menza C (1999) The biochemical pathway of neurofibrillary degeneration in aging and Alzheimer's disease. *Neurology* 2:1158-1165.
7. Gallyas F (1971) Silver staining of Alzheimer's neurofibrillary changes by means of physical development. *Acta Morphol Acad Sci Hung* 19:1-8.
8. Gervais F, Xu D, Robertson GS, Vaillancourt J, Zhu Y, Vaillancourt JP, Zhu Y, Huang J, LeBlanc A, Smith D, Rigby M et al (1999) Involvement of caspase in proteolytic cleavage of Alzheimer's disease amyloid-b precursor protein and amyloidogenic Aβ peptide formation. *Cell* 97:395-406.
9. Gomez-Isla T, Hollister R, West H, Mui S, Growdon JH, Petersen RC, Parisi JE, Hyman BT (1997) Neuronal loss correlates with but exceeds neurofibrillary tangles in Alzheimer's disease. *Ann Neurol* 41:17-24.
10. Grant SM, Ducatenzeiler A, Szyf M, Cuello AC. (2000) Aβ immunoreactive material is present in several intracellular compartments in transfected neuronally differentiated, P19 cell expressing the human amyloid-precursor protein. *Journal of Alzh Dis* 2:207-222.
11. Guo Q, Fu W, Xie J, Luo H, Sells SF, Geddes JW, Bondada V, Rangnekar VM, Mattson MP (1998) Par-4 is a mediator of neuronal degeneration associated with the pathogenesis of Alzheimer disease. *Nat Med* 4:957-962.
12. Guo Q, Sopher BL, Furukawa K, Pham DG, Robinson N, Martin GM, Mattson MP (1997) Alzheimer's presenilin mutation sensitizes neural cells to apoptosis induced by trophic factor withdrawal and amyloid beta-peptide: involvement of calcium and oxyradicals. *J Neurosci* 17:4212-4222.
13. Ivins KJ, Thornton PL, Rohn TT, Cotman CW (1999) Neuronal apoptosis induced by beta-amyloid is mediated by caspase-8. *Neurobiol Dis* 6:440-449.
14. Kitamura Y, Shimoshama S, Kamoshima W, Ota T, Matsuoka Y, Nomura Y, Smith MA, Perry G, Whitehouse PJ, Taniguchi T (1998) Alteration of proteins regulating apoptosis: bcl-2, bcl-x, bax, bak,bad, ICH-1, and CPP32 in Alzheimer's disease. *Brain Research* 780:260-269.
15. Kitamura Y, Taniguchi T, Shimohama S (1999) Apoptotic cell death in neurons and glial cells: implications for Alzheimer's disease. *Jpn J Pharmacol* 79:1-5.
16. Lassmann H, Bancher C, Breitschopf H, Wegiel J, Bobinski M, Jellinger K, Wisniewski HM (1995) Cell death in Alzheimer's disease evaluated by DNA fragmentation in situ. *Acta Neuropathol (Berl)* 89:35-41.
17. Lu DC, Rabizadeh S, Chandra S, Shayya RF, Ellerby LM, Ye X, Salvesen GS, Koo EH, Bredesen DE (2000) A second cytotoxic proteolytic peptide derived from amyloid beta-protein precursor. *Nat Med* 6:397-404.
18. Lucassen PJ, Chung WC, Kamphorst W, Swaab DF (1997) DNA damage distribution in the human brain as shown by in situ end labeling; area-specific differences in aging and Alzheimer disease in the absence of apoptotic morphology. *J Neuropathol Exp Neurol* 56:887-900.
19. Marks N, Berg MJ (1999) Recent advances on neuronal caspases in development and neurodegeneration. *Neurochem Int* 35:195-220.
20. Masliah E, Mallory M, Alford M, Tanaka S, Hansen LA (1998) Caspase dependent fragmentation might be associated with excitotoxicity in Alzheimer disease. *J Neuropathl Exp Neurol* 57:1041-1052.
21. Mattson MP, Duan W, Pedersen WA, Culmsee C (2001) Neurodegenerative disorders and ischemic brain diseases. *Apoptosis* 6:69-81.
22. Neve RL, McPhie DL, Chen Y (2000) Alzheimer's disease: a dysfunction of the amyloid precursor protein. *Brain Res* 886:54-66.
23. Nijhawan D, Honarpour N, Wang X (2000) Apoptosis in neural development and disease. *Annu Rev Neurosci* 23:73-87.
24. Nishimura T, Akiyama H, Yonehara S, Kondo H, Ikeda K, Kato M, Iseki E, Kosaka K (1995) Fas antigen expression in brains of patients with Alzheimer-type dementia. *Brain Res* 95:137-145.
25. Pellegrini L, Passer BJ, Tabaton M, Ganjei JK, D'Adamio L (1999) Alternative, non-secretase processing of Alzheimer's beta-amyloid precursor protein during apoptosis by caspase-6 and -8. *J Biol Chem* 274:21011-21016.
26. Perry G, Nunomura A, Smith MA (1998) A suicide note from Alzheimer disease neurons? *Nat Med* 4(8):957-962.

27. Robertson GS, Crocker SJ, Nicholson DW, Schulz JB (2000) Neuroprotection by the inhibition of apoptosis. *Brain Pathol* 2:283-292.
28. Rohn TT, Head E, Su JH, Anderson AJ, Bahr BA, Cotman CW, Cribbs DH (2001) Correlation between caspase activation and neurofibrillary tangle formation in Alzheimer's disease. *Am J Pathol* 158:189-198.
29. Selznick LA, Holtzman DM, Han BH, Gokden M, Srinivasan AN, Johnson EM Jr, Roth KA (1999) In situ immunodetection of neuronal caspase-3 activation in Alzheimer disease. *J Neuropathl Exp Neurol* 58:1020-1026.
30. Selznick LA, Zheng TS, Flavell RA, Rakic P, Roth KA (2000) Amyloid beta-induced neuronal death is bax-dependent but caspase-independent. *J Neuropathl Exp Neurol* 59:271-279.
31. Shimohama S, Tanino H, Fujimoto S (1999) Changes in caspase expression in Alzheimer's disease: comparison with development and aging. *Biochem Bioph Res Comm* 256:381-384.
32. Smale G, Nichols NR, Brady DR, Finch CE, Horton WE Jr (1995) Evidence for apoptotic cell death in Alzheimer's disease. *Exp Neurol* 133:225-230.
33. Stadelmann C, Deckwerth TL, Srinivasan A, Bancher C, Bruck W, Jellinger K, Lassmann H (1999) Activation of caspase-3 in single neurons and autophagic granules of granulovacuolar degeneration in Alzheimer's disease. Evidence for apoptotic cell death. *Am J Pathol* 155:1459-1466.
34. Stadelmann C, Bruck W, Bancher C, Jellinger K, Lassmann H (1998) Alzheimer disease: DNA fragmentation indicates increased neuronal vulnerability, but not apoptosis. *J Neuropathl Exp Neurol* 57:456-464.
35. Su JH, Zhao M, Anderson AJ, Srinivasan A, Cotman CW (2001) Activated caspase-3 expression in Alzheimer's and aged control brain: correlation with Alzheimer pathology. *Brain Res* 898:350-357.
36. Su JH, Deng G, Cotman CW (1997) Neuronal DNA damage precedes tangle formation and is associated with upregulation of nitrotyrosine in Alzheimer's disease brain. *Brain Res* 774:193-199.
37. Su JH, Anderson AJ, Cummings BJ, Cotman CW (1994) Immunohistochemical evidence for apoptosis in Alzheimer's disease. *Neuroreport* 5:2529-2533.
38. Terry RD (2000)Cell death or synaptic loss in Alzheimer disease. *J Neuropathol Exp Neurol* 59:1118-1119.
39. Terry RD (2001) An honorable compromise regarding amyloid in Alzheimer disease. *Ann Neurol* 49:684.
40. Troncoso JC, Sukhov RR, Kawas CH, Koliatsos VE (1996) In situ labeling of dying cortical neurons in normal aging and in Alzheimer's disease: Correlation with senile plaques and disease progression. *J Neuropathol Exp Neurol* 55:1134-1142.
41. Tsang SY, Tam SC, Bremner I, Burkitt MJ (1996) Copper-1,10-phenanthroline induces internucleosomal DNA fragmentation in HepG2 cells, resulting from direct oxidation by the hydroxyl radical. Biochem J 317:13-16.
42. Wolozin B, Iwasaki K, Vito P, Ganjei JK, Lacana E, Sunderland T, Zhao B, Kusiak JW, Wasco W, D'Adamio L (1996) Participation of presenilin 2 in apoptosis: enhanced basal activity conferred by an Alzheimer mutation. Science 274:1710-1713.
43. Yamatsuji T, Matsui T, Okamoto T, Komatsuzaki K, Takeda S, Fukumoto H, Iwatsubo T, Suzuki N, Asami-Odaka A, Ireland S, Kinane TB, Giambarella U, Nishimoto I (1996) G protein-mediated neuronal DNA fragmentation induced by familial Alzheimer's disease-associated mutants of APP. *Science* 272:1349-1352.
44. Yang F, Sun X, Beech W, Teter B, Wu S, Sigel J, Vinters HV, Frautschy SA, Cole GM (1998) Antibody to caspase-cleaved actin detects apoptosis in differentiated neuroblastoma and plaque-associated neurons and microglia in Alzheimer's disease. *Am J Pathol* 152:379-389.
45. Yuan J, Yankner BA (2000) Apoptosis in the nervous system. *Nature* 407:802-809.
46. Zheng TS, Hunot S, Kuida K, Momoi T, Srinivasan A, Nicholson DW, Lazebnik Y, Flavell RA (2000) Deficiency in caspase-9 or caspase-3 induces compensatory caspase activation. *Nat Med* 11:1241-1247.